TECHNISCHE UNIVERSITÄT WIEN

*Variational Analysis, Dynamics and Operations Research*

SWM VADOR

# A spatial epidemiological model with contact and mobility restrictions

F. Ferraccioli, N. I. Stilianakis, V. M. Veliov

**Research Report 2023-02**

November 2023

ISSN 2521-313X

**Variational Analysis, Dynamics and Operations Research**
Institute of Statistics and Mathematical Methods in Economics
TU Wien

Research Unit VADOR
Wiedner Hauptstraße 8 / E105-04
1040 Vienna, Austria
E-mail: vador@tuwien.ac.at

# A spatial epidemiological model with contact and mobility restrictions*

Federico Ferraccioli[†‡], Nikolaos I. Stilianakis[§¶‖], Vladimir M. Veliov[**]

**Abstract**

Several spatiotemporal epidemiological models have described how contact and mobility restrictions have a dynamic effect on morbidity and mortality of fast transmitting pathogens in epidemics. Despite this, there has been rather limited contributions looking at policy optimization. This work combines a new spatiotemporal epidemiological model of a heterogeneous mixed population located at different places with an optimal control approach to show the effects of contact and mobility restrictions under policy optimization. The objective of optimization not only includes epidemiological but also socio-economic implications of the restrictions. Several scenarios are numerically investigated and the dependence of the optimal policy on some basic epidemiological parameters is analyzed. The results illustrate the strong impact of the spatial heterogeneity on the optimal policy measures. Analysis of the stability of the disease free equilibrium of the model is also presented.

**Keywords:** spatial model, infectious diseases, epidemics, contacts, travel

## 1 Introduction

Considering spatially heterogeneous mixing and interventions in infectious disease epidemiological modelling is essential. Human mobility and its effects on contact patterns geographically plays a key role in the transmission of pathogens to humans especially in the case of airborne infectious pathogens such as influenza and corona viruses. The general concepts in heterogeneity of host population in epidemiological models have been described in the literature (Hethcote [1]; Brauer et al. [2]) with further developed concepts that include mobility and indirect transmission (Castillo-Chavez et al. [3], David et al. [4]).

One way to model human mobility with heterogeneous mixing and the impact on airborne pathogen transmission is to divide the population in subgroups with different activity levels.

*This research is supported by the Austrian Science Fund (FWF) under grant No I-4571-N.

[†]European Commission, Joint Research Centre (JRC), Ispra, Italy.

[‡]Current address: Department of Statistical Sciences, Padua University, Italy. federico.ferraccioli@unipd.it

[§]European Commission, Joint Research Centre (JRC), Ispra, Italy

[¶]Department of Biometry and Epidemiology, University of Erlangen-Nuremberg, Erlangen, Germany. nikolaos.stilianakis@ec.europa.eu Disclaimer: The views expressed are purely those of the writer (NIS) and may not in any circumstance be regarded as stating an official position of the European Commission.

[‖]Corresponding author

[**]Institute of Statistics and Mathematical Methods in Economics, Vienna University of Technology, Austria, vladimir.veliov@tuwien.ac.at.

David and Iyaniwura [5] consider a Susceptible-Infected-Removed (SIR)-type model at each place of residence and use a coupled partial differential equations (PDE)-ordinary differential equations (ODE) system to study the effects of human mobility on airborne pathogen transmission in a heterogeneously mixed population setting. By doing so they can track the epidemic development at an individual's place of residence at any time. The corresponding transmission mechanism of the pathogen is diffusion. The authors obtain a flattening epidemic curve as the diffusion rate of the pathogen increases. Zhang and Jin [6] introduce a model with two geographical areas interconnected due to travel between the areas. The reproduction numbers and the final state of the disease are investigated depending on the contact rate and probability of early diagnostics. Bertaglia et al. [7] develop a spatial multiscale model with transport of commuters and diffusion of non-commuters in urban areas using data from Italy.

With a reaction–diffusion system Chen et al. [8] define distance based on the mobility network among various locations. In the network the weights of the edges between pairs of locations are the relative population flow among them. The authors select sub-regions in epidemic areas with active population movements and derive solutions to initiate new travel flows among the sub-regions. Applying their approach to Corona Virus Disease of 2019 (COVID-19) they find that lifting travel restrictions based on their solutions will not cause a new epidemic wave. Geng et al. [9] use a kernel-modulated SIR modelling approach to characterize the dynamic of Severe Acute Respiratory Syndrome Coronavirus (SARS-CoV-2) in a multifractal distributed susceptible population. The model reproduced multiphase COVID-19 epidemics and explained the fact that while the reproduction number was reduced due to interventions such as social distancing, subsequent epidemic waves still occurred. This was attributed to an increase in susceptible population flow following a relaxation of travel restrictions. Grimee et al. [10] use a spatiotemporal extension of a multivariate time series model that additively decomposes incidence into an endemic and an epidemic component. The epidemic component captures incidence driven by previous case counts, and the endemic component captures exogenous contributions to incidence such as seasonal factors. Spatial dependencies are captured by neighbourhood matrices adjusted over time to reflect changes in spatial connectivity between geographical areas. The approach applied to COVID-19 with data and indicators describing mobility patterns and travel restrictions. Scenarios of border closures and their effects on the number of cases were studied.

Meta-population dynamical models have also been used to capture the spatiotemporal transmission of SARS-CoV-2. Aguilar et al. [11] employed a meta-population framework to show the role of urban flows in infectious disease spreading. They find that cities where flows are between hotspots show high vulnerability to the rapid spread of the pathogen with mobility restrictions to be effective in controlling the epidemic. Sprawled cities show a slower spread of the pathogens but with a weaker effect of mobility restrictions such as population travel. In an application in China provinces the spatial diffusion of the infection was captured by parameterizing human mobility (Jia et al. [12]). Rapti et al. [13] developed also a meta-population model incorporating mobility across the province nodes of Andalusia in Spain using mobile-phone time-dependent data. Mazzoli et al. [14] looked within a similar meta-population framework at the contribution of multi-seeding in association with mobility and lock-downs and how they affect the local transmission of SARS-CoV-2. In a meta-population model based on temporal networks Parino et al. [15] use COVID-19 data in Italy to investigate reduced social activity and mobility restrictions. They show that the effects of mobility restrictions strongly depends on timely contact and mobility restrictions in the early phases of the outbreak. They argue in favor of social activity reduction policies afterwards. In a geo-hierarchical model Topirceanu and Precup [16] incorporate the

spatial distribution of hierarchically structured population into geographical settlements. They model the movement of individuals using travel distance and frequency parameters for inter and intra-settlement movement. A SIR type model reproduces high variation in size and temporal heterogeneity. Epidemic size was more sensitive to increased distance of travel than frequency of travel. Uiterkamp et al. [17] investigated under which epidemiological conditions incorporating mobility into transmission models improves forecasting. The authors utilized a simple mobility-enhanced SEIR compartmental model with commuter information at the municipality level. Inter-regional mobility consideration generally led to an improvement in forecast quality. When policies were in place that aimed to reduce contacts or travel, this improvement was very small. The improvement became larger when municipalities had a relatively large amount of incoming mobility compared with the number of inhabitants.

In an epidemic model Nakata and Roest [18] describe the effects of transportation networks consisting of heterogeneous regions on pathogen transmission during transportation. Using stability theory of delay differential equations, theory of asymptotically autonomous semiflows and cooperative sublinear dynamical systems they show that for weakly connected transportation networks endemic patterns exist with a globally asymptotically stable equilibrium, which may be disease free in some regions while endemic in other regions. Spatial heterogeneity with different basic reproduction numbers they may depend non-monotonically on the dispersal rates indication that travel restrictions may not always be beneficial.

In many of these studies the effects of control strategies were studied but no policy optimization was attempted. This is also a general observation in the corresponding literature. The approach presented here is similar to David et al. [5] with the novel element of considering policy optimization.

The aim of this work is to study policy strategies for the control of epidemics and in particular fast unfolding outbreaks of aerially transmitted pathogens such as SARS-CoV-2 or influenza. The paper is structured as follows. In section 2 we describe the SIR type model with its spatial characteristics assuming proportional random mixing of the population. In addition, we extend the model and introduce two types of control policies. First, we look at the effects of contact restrictions at place $x$ that do not affect business continuity. Second, we explore the scenario of mobility restriction, e.g., traveling from place $x$ to place $y$ having consequences for business continuity. In section 3 we perform stability analysis of the disease free equilibrium and calculate the basic reproduction number. The optimization of the policy measures towards minimization of the number of deaths, under explicit consideration of the socio-economic costs caused by the policy measures, is presented in section 4. Corresponding numerical results and analysis of the dependence of the optimal policy and the evolution of the epidemic on some basic model parameters are given in section 5. In section 6 we provide a discussion of the results also in the sense of potential implications for policy making.

## 2 The basic model and its control extension

We consider a geographical region $\Omega$ consisting of $M$ cities (further called locations), denoted by $x_1, \ldots, x_M$. The population at each location consists of three groups: $S(t, x)$ is the size of the susceptible population at location $x \in \Omega$ and time $t$; $I(t, x)$ and $R(t; x)$ are the respective sizes of the infected and the recovered subpopulations. Correspondingly, the model proposed below

represents a spatial extension of the usual SIR epidemiological model.[1] The main parameters of the model are:

$\iota$ – force of infection,
$\rho$ – recovery rate,
$\nu$ – rate of transition from recovered to susceptible due to waning immunity,
$\mu$ – mortality rate due to disease,
$c(t,x)$ – contact rate at location $x$ (to be taken independent of $t$, thus ignoring seasonal changes),
$\alpha(t)$ – fraction of the infected individuals participating in contacts (activity rate of infected),
$\sigma(x,y)$ – fraction of residents of location $x$ who visit location $y \in \Omega$ per unit of time.

"Visits" may be due to work, shopping, tourism, etc. The parameter $\sigma(x,y)$ should take into account the time that residents of $x$ spend at $y$. If a "visits" from $x$ to $y$ is due to work, then only about a half of the (active) time is spent at $y$, the other half is spent at $x$. If a visit is for shopping, for example, then only a smaller fraction of the time is spent at $y$. If a visit is for vacation, then all the time is spent at $y$. Thus, $\sigma(x,y)$ does not just reflect the number of visits from $x$ to $y$ per day; all the above information has to be incorporated in the parameter $\sigma$. Of course, $\sum_{y\in\Omega}\sigma(x,y)=1$ for every $x$.

Similarly as in the SIR model, the dynamics of the epidemics on a time interval $[0,T]$ is described by the equations

$$\frac{\mathrm{d}}{\mathrm{d}t}S(t,x) = -\sum_{y\in\Omega} c(t,y)D(t,y)\sigma(x,y)S(t,x) + \nu R(t,x), \qquad S(0,x)=S_0(x), \tag{2.1}$$

$$\frac{\mathrm{d}}{\mathrm{d}t}I(t,x) = \sum_{y\in\Omega} c(t,y)D(t,y)\sigma(x,y)S(t,x) - (\rho+\mu)I(t,x), \qquad I(0,x)=I_0(x), \tag{2.2}$$

$$\frac{\mathrm{d}}{\mathrm{d}t}R(t,x) = -\nu R(t,x) + \rho I(t,x), \qquad R(0,x)=R_0(x), \tag{2.3}$$

with $t\in[0,T]$, $x\in\Omega$, where $D(t,y)$ is the infectiousness (risk of getting infected) at locations $y$. Assuming proportional random mixing it takes the form

$$D(t,y) = \iota \frac{\sum_{z\in\Omega}\sigma(z,y)\alpha(t,z)I(t,z)}{\sum_{z\in\Omega}\sigma(z,y)(S(t,z)+R(t,z)+\alpha(t,z)I(t,z))}. \tag{2.4}$$

Notice that $\alpha(t)$ may be influenced by policy, for example by testing, which allows people to know they are infected before appearance of symptoms, hence to decrease $\alpha$. For this reason we allow dependence of $\alpha$ on time.

The model can be extended by introducing two types of policies (in addition to $\alpha$, which will be only used for comparative analysis). The first one, denoted by $u(t,x)\in[u_0,1]$, is a restriction of the contacts at place $x$ without affecting the business activities. It may take the form of various policies of wearing masks, restrictions for visiting public places, etc. A value $u(t,x)<1$ means reduction of the contacts to a fraction $u(t,x)$ of the normal ones. In contrast, a second policy variable, $v(t,y)\in[v_0,1]$, restricts the business activities at $y$ to a fraction $v(t,y)$ of the

[1] More compartments can be involved in the model for more detailed description of the disease dynamics, similarly as in the single location models.

normal one. As a result, also the travel intensity to $y$ reduces by the same fraction, therefore we identify this restriction with travel (mobility) restriction. For example, if factories at $y$ close then commuting for work to $y$ will be reduced; if hotels at a touristic location close then touristic visits to $y$ will reduce proportionally, etc. As a result of the traveling restrictions, an additional fraction $(1 - v(t, y))\sigma(x, y)$ of residents of $x$ visiting $y$ (in case of no restrictions) will stay at $x$. We also mention that the control $v(t, y)$ restricts entering location $y$ but not leaving it. The latter kind of restrictions can also be easily modeled, which is not done in this paper.

In summary, we have the following control variables:

- Contact (social) restrictions at $x$ : $u(t, x)$, with $u : [0, T] \times \Omega \to [u_0, 1]$, where $0 < u_0 < 1$;
- Partial lock-down at $y$ (which leads to less travel to $y$ for work, touristic/vacation visits, shopping, etc.): $v(t, y)$, with $v : [0, T] \times \Omega \to [0, 1]$.

In order to formulate the extended model in a more convenient way we introduce some notations. It is assumed that individuals who instead of visiting a remote location stay at their place of residence due to a lock-down at the other location, have a contact rate reduced by a factor $\beta \in [0, 1]$. Then we define

$$\psi(t, x, y) := \begin{cases} v(t, y)\sigma(x, y) & \text{for } y \neq x, \\ v(t, x)\sigma(x, x) + \beta \sum_{\xi \in \Omega}(1 - v(t, \xi))\sigma(x, \xi) & \text{for } y = x, \end{cases}$$

which is the fraction of residents of $x$ visiting $y$, given the lock-down policy $v(t, \cdot)$, thus the value $\psi(t, x, y)$ has to replace $\sigma(x, y)$ in (2.1), (2.2) and (2.4). Moreover, we abbreviate $E(t, x) = (S(t, x), I(t, x), R(t, x))$. The overall controlled epidemic dynamics takes the form

$$\frac{\mathrm{d}}{\mathrm{d}t}S(t, x) = -G(t, x, E(t, \cdot))\, S(t, x) + \nu R(t, x), \tag{2.5}$$

$$\frac{\mathrm{d}}{\mathrm{d}t}I(t, x) = G(t, x, E(t, \cdot))\, S(t, x) - (\rho + \mu)I(t, x), \tag{2.6}$$

$$\frac{\mathrm{d}}{\mathrm{d}t}R(t, x) = -\nu R(t, x) + \rho I(t, x). \tag{2.7}$$

where

$$G(t, x, E(t, \cdot)) := \sum_{y \in \Omega} u(t, y)c(t, y)D(t, y, E(t, \cdot))\psi(t, x, y),$$

and

$$D(t, y, E(t, \cdot)) := \iota\alpha(t)\frac{\sum_{z \in \Omega} \psi(t, z, y)I(t, z)}{\sum_{z \in \Omega} \psi(t, z, y)(S(t, z) + R(t, z) + \alpha(t)I(t, z))}.$$

Although the functions $D$ and $G$ depend on the time $t$, sometimes we we suppress $t$ in the notations. Similarly, $\psi(t, x, y)$ depends on $v(t, y)$, thus $D$ depends on $v(t, \cdot)$, $G$ depends on $v(t, \cdot)$ and $u(t, \cdot)$, which is not explicit in the notations..

Throughout the paper we assume that the data listed at the beginning of Section 2 are nonnegative and continuous in $t$, the components of $E(0, x)$ are nonnegative, $S(0, x) + I(0, x) + R(0, x) > 0$ for each $x \in \Omega$.

## 3 Stability of the disease free equilibrium and basic reproduction numbers

To investigate the stability of the disease free equilibrium we assume that all data $c(x)$, $\sigma(x,y)$, $u(x)$, $v(x)$, $\alpha$, with $x, y \in \Omega$, are time-invariant. Consider an equilibrium $\hat{E} := (\hat{S}, 0, \hat{R})$ with $\hat{S}(x) + \hat{R}(x) > 0$ for all $x \in \Omega$.

The Jacobian of the right–hand side of (2.5)–(2.7) at $\hat{E}$, denoted further by $\mathcal{J}$, is a $(3M \times 3M)$-matrix. Obviously $D(y, \hat{E}(\cdot)) = 0$, hence $G(x, \hat{E}(\cdot)) = 0$ for all $x, y \in \Omega$. By a direct inspection we see that

$$\frac{\partial D(x_j, E(\cdot))}{\partial S(x_k)}\Big|_{E=\hat{E}} = 0, \quad \text{hence} \quad \frac{\partial G(x_i, E(\cdot))}{\partial S(x_j)}\Big|_{E=\hat{E}} = 0, \quad i,j,k \in \{1,\dots,M\}.$$

Moreover, the right-side of (2.7) is independent of $S$. Hence, the first $M$ columns of $\mathcal{J}$ are zero. In addition, similarly as above

$$\frac{\partial G(x_i, E(\cdot))}{\partial R(x_j)}\Big|_{E=\hat{E}} = 0, \quad i,j \in \{1,\dots,M\}.$$

Thus the matrix $\mathcal{J}$ has the following structure:

$$\mathcal{J} = \begin{pmatrix} 0 & P & \nu\mathcal{I} \\ 0 & J & 0 \\ 0 & \rho\mathcal{I} & -\nu\mathcal{I} \end{pmatrix}, \tag{3.1}$$

where $\mathcal{I}$ is the identity matrix of dimension $M$, $P$ is matrix of no interest, $J$ has components

$$\frac{\partial\big(G(x_i, E(\cdot))\, S(x_i) - (\rho+\mu) I(x_i)\big)}{\partial I(x_j)}\Big|_{E=\hat{E}}.$$

One can express

$$\frac{\partial G(x_i, E(\cdot))}{\partial I(x_j)}\Big|_{E=\hat{E}} = \sum_{k=1}^{M} u(x_k) c(x_k) \frac{\partial D(x_k, \hat{E}(\cdot))}{\partial I(x_j)} \psi(x_i, x_k).$$

and

$$\frac{\partial D(x_k, E(\cdot))}{\partial I(x_j)}\Big|_{E=\hat{E}} = \iota\alpha \frac{\psi(x_j, x_k)}{B(x_k)}, \qquad \text{where} \;\; B(x_k) := \sum_{s=1}^{M} \psi(x_s, x_k)(\hat{S}(x_s) + \hat{R}(x_s)),$$

Hence,

$$J = A - (\rho+\mu)\mathcal{I},$$

where $A$ has the entries

$$a_{ij} := \iota\alpha \sum_{k=1}^{M} u(x_k) c(x_k) \frac{\psi(x_j, x_k)}{B(x_k)} \psi(x_i, x_k) \hat{S}(x_i), \quad i,j \in \{1,\dots,M\}. \tag{3.2}$$

Having in mind (3.1) we obtain that $\mathcal{J}$ has $M$ eigenvalues equal to zero (corresponding to the $S$-variables), $M$ eigenvalues equal to $-\nu$ (corresponding to the $R$-variables), and the other $M$ are the eigenvalues of $J$.

For the spectrum of $J$ we obviously have that $\operatorname{sp} J = \operatorname{sp} A - (\rho+\mu)$. The matrix $A$ is symmetric, therefore its eigenvalues are real. Thus the eigenvalues of $\mathcal{J}$ corresponding to the $I$-variables are negative if and only if

$$\kappa < (\rho + \mu) \quad \text{for all } \kappa \in \operatorname{sp} A. \tag{3.3}$$

Under this condition $I(t,x)$ exponentially converges to zero if $I_0(x) \geq 0$ is sufficiently small. This proves the following proposition.

**Proposition 3.1.** *Under the assumptions made for the data and* (3.3)*, any solution* $(S(\cdot), I(\cdot), R(\cdot))$ *starting from* $(S(0,\cdot), I(0,\cdot), R(0,\cdot))$ *being sufficiently close to* $(\hat{S}, 0, \hat{R})$ *converges to a disease-free equilibrium* $(\bar{S}, 0, \bar{R})$*. If* $\mu = 0$ *and* $\nu > 0$*, then* $\bar{S} = \hat{S} + \hat{R}$*, and* $\bar{R} = 0$*. The basic reproduction number equals*

$$\mathcal{R} = e^{\max\{\operatorname{sp} A\} - (\rho+\mu)}. \tag{3.4}$$

The statement of the proposition in the case $\mu = 0$ follows from the fact that in this case the total population at each location remains constant.

From the formula (3.2) for the coefficient of the matrix $A$ it is clear that the elements of its spectrum are small enough to ensure $\mathcal{R} < 1$ if the values of $\alpha$ or $c$ or $u$ are small enough. In particular, if more testing (small $\alpha$) or stricter contact restriction (small $u$) are applied, then (3.3) is fulfilled and the basic reproduction number is smaller than one. The same does not apply to the lock-down control $v$.

We also mention that in the case of a single location ($M = 1$) the expression (3.4) for the basic reproduction number coincides with the known one for the SIR model.

# 4 Optimization of the policy measures

In this section, we consider an optimal control problem where the goal is to minimize the total number of deaths (or hospitalizations) on a given time interval $[0, T]$, regarding at the same time the costs caused by the disease and the policy measures. The social contact restriction $u(t,x)$ and the partial lock-down $v(t,x)$ will be considered as control (policy) variables. The number of deaths at time $t$ is $\mu \sum_{x\in\Omega} I(t,x)$. The economic component of the model (needed especially if lock-down measures $v$ are taken, because these measures critically influence the economic output) is deliberately taken in a very simple form, compared with the existing literature, i.e. Bloom et al. [19] or Caulkins et al. [20]. The productivity of the population is denoted by $\pi$, so that the economic output at place $x$ and time $t$ is

$$\pi v(t,x) \sum_{y\in\Omega} \sigma(y,x)(S(t,y) + R(t,y) + \alpha(t) I(t,y)).$$

The contact restrictions, $u(t,x) \leq 1$, and the (partial) lock-down, $v(t,x) \leq 1$, create social disutility assumed in the form

$$\varepsilon_u (1 - u(t,x))^2 + \varepsilon_v (1 - v(t,x))^2, \qquad \varepsilon_u, \varepsilon_v \geq 0.$$

These terms represent the public pressure applied to the decision maker due to the inconvenience and the violation of freedom (caring masks, restrictions on social events and the size of private

meetings, etc.) caused by policy measures. Therefore, we define (after change of the order of summation) the "running cost" of the epidemics as

$$\begin{aligned} F(E(t,\cdot),u(t,\cdot),v(t,\cdot)) &= \sum_{x\in\Omega}\big[-L\,\mu I(t,x)+\pi\left(S(t,x)+R(t,x)+\alpha(t)I(t,x)\right)\sum_{y\in\Omega}v(t,y)\sigma(x,y) \\ &\quad -\varepsilon_u(1-u(t,x))^2-\varepsilon_v(1-v(t,x))^2\big] \end{aligned}$$

where $L>0$ is a weighting parameter representing the value the decision maker attributes to human life. Then the considered optimal control problem takes the form

$$\max_{u,v}\int_0^T e^{-rt}F(E(t,\cdot),u(t,\cdot),v(t,\cdot))\,\mathrm{d}t, \tag{4.1}$$

subject to the equations (2.5)–(2.7) and the control constraints $u(t,x)\in[u_0,1]$, $v(t,x)\in[v_0,1]$. Here, $r\geq 0$ is a discount factor. Discounting the number of deaths is due to the expectation that the probability of dying from infection decreases due to the progress in the medical treatment with time. Discounting the economic and the social disutility components of the objective functional is typical in economics. The two discount rates can differ from each other, but in the present paper they are assumed equal for simplicity.

Due to the discrete nature of the spacial domain $\Omega$, the optimal control problem (2.5)–(2.7), (4.1) is standard, and optimality conditions (the Pontryagin maximum principle) are known. However, the problem is too complicated to be investigated analytically. Here, we only mention that if $v$ is fixed and only $u$ is used as a control variable, existence and uniqueness of an optimal solution follows in a standard way from the linearity of the equations and the concavity of the objective functional with respect to $u$. Existence of a solution of the problem where also $v$ is considered as a control is not obvious. For the numerical solutions presented in the next section we use our own software based on the gradient projection method in the control space. The gradient of the objective functional with respect to the control functions in the space $L^\infty(0,T)$ is approximately calculated by solving the corresponding adjoint equation, for which a second order Runge-Kutta discretization method (the Heun scheme) is utilized. A justification of the applied discretization technique for optimal control problems is given in Dontchev et al. [21].

## 5 Computer simulation and optimization

We begin with the description of a benchmark configuration that we use in the numerical study. We consider a geographical region consisting of three locations with total population size 100. The locations, denoted by **A**, **B**, and **C** have sizes 60, 20 and 20, correspondingly. Presumably, **A** is an industrial city, **B** is a smaller city close to **A**, so that many people from **B** visit **A** for work, shopping, etc. City **C** is presumably a resort town with many visitors, dominantly from **A**. Correspondingly, the matrix of the population flow between the three cities is

$$\sigma=\begin{pmatrix} 0.95 & 0 & 0.05 \\ 0.15 & 0.83 & 0.02 \\ 0.01 & 0 & 0.99 \end{pmatrix},$$

The time unit is one day. We consider the scenario where at time zero there is an infected subpopulation of **C** of size 3. Therefore, the initial data for the model is

$$S_0=(60,20,17),\quad I_0=(0,0,3),\quad R_0=(0,0,0).$$

The remaining parameter values are listed below:
$c(t,\cdot,) = \hat{c}\,(12, 4, 15)$ with $\hat{c} = 0.4$,
$\rho = 1/15$ (the average duration of infection is 15 days),
$\nu = 1/180$ (the average period of immunity after infection is 180 days),
$\mu = -\ln(0.975)\rho$, which corresponds to 2.5% deaths per infection ($\mu \approx 0.0017$),
$\iota = 0.1$,
$\alpha = 0.4$,
$L = 200$,
$\pi = 0.002$,
$\varepsilon_u = 2$,
$\varepsilon_v = 0.05$,
$r = 0$.

The control constraints for the optimization are $u, v \in [0.4, 1]$, that is $u_0 = v_0 = 0.4$. The choice of the parameters $\rho, \nu, \mu, \iota, \alpha$ is appropriate for COVID-19, parameters $c(\cdot)$ are consistent with $\iota$, the other parameters concern the objective functional and mainly have meaning as weights.

Numerically obtained results about the benchmark case, as well as for various its modifications follow. In all plots, lines in read/green/blue correspond to cities A/B/C.

**1.** The basic reproduction number for the benchmark case (neglecting the mortality, i.e. $\mu = 0$) is 1.1574, and the epidemic converges to an endemic state. Infected individuals at the endemic state are located as follows: 5% of the local population at city A, 3% at city B, and 6% at city C. Only a few oscillations are visible in the long run on Figure 5.1. The basic reproduction number can be decreased to values below 1 by contact restrictions that, for example, are constant in time and are the same for all locations, by implementing control $u(x,t) = u < 0.313$. The evolution of the epidemic can be influenced and the reproduction number can be reduced by decreasing the parameter $\alpha$. As explained in Section 2, this parameter depends on the testing intensity which allows for early identification of infection of individuals. The parameter $\alpha$ can be used as an additional time-varying control variable, the effect of which is seen on Figure 5.2. The effect of testing is particularly high in the first pick of the disease.

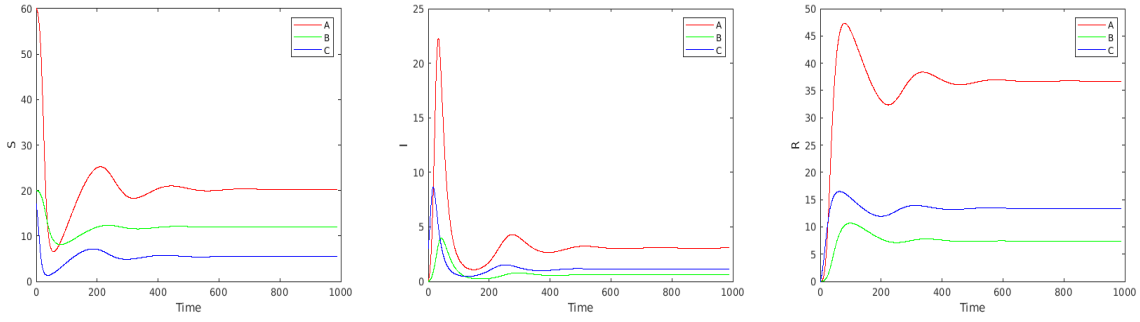


Figure 5.1: Endemic case in the long run (with $\mu = 0$). Left to right $S$, $I$, $R$.

**2.** Next, we consider the optimal solutions of problem (2.5)–(2.7), (4.1) in the benchmark case. The first two plots on Figure 5.3 present the optimal controls; the corresponding $S$, $I$ and $R$

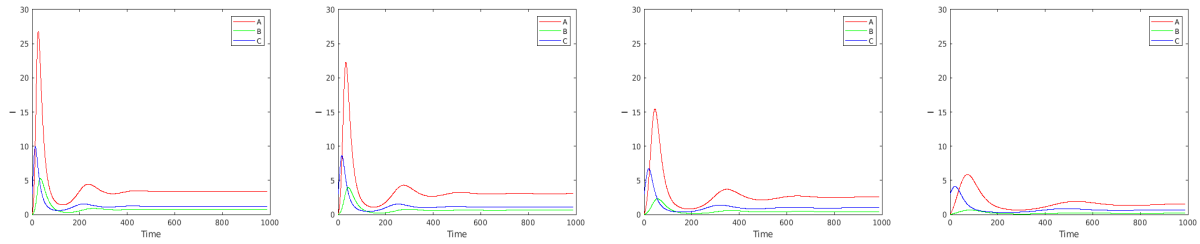


Figure 5.2: Evolution of $I$ (with $\mu = 0$) for values of $\alpha = 0.5, 0.4, 0.3, 0.2$ (left to right).

are given in the second three plots. Looking at the plot of $u$, it is remarkable that in the first days of the epidemic the optimal contact restriction at the "touristic" location C (where the epidemic begins, as in Austria, for example) is extremely high while the contact restrictions become persistently stronger in the big city A after about 20 days. The reason is that the disease quickly moves from the small city C to the large one, A. In contrast, the partial lock-down, $v$, is negligible at A, and that at C is (again) strong at the beginning and during the second wave of the disease after day 250.

Comparing the trajectories on Figures 5.3 and 5.4 we see that in the benchmark case the lock-down control $v$ plays a relatively minor role for the epidemic. Therefore in the subsequent experiments we use only $u$ as a control variable, fixing $v(t) = 1$.

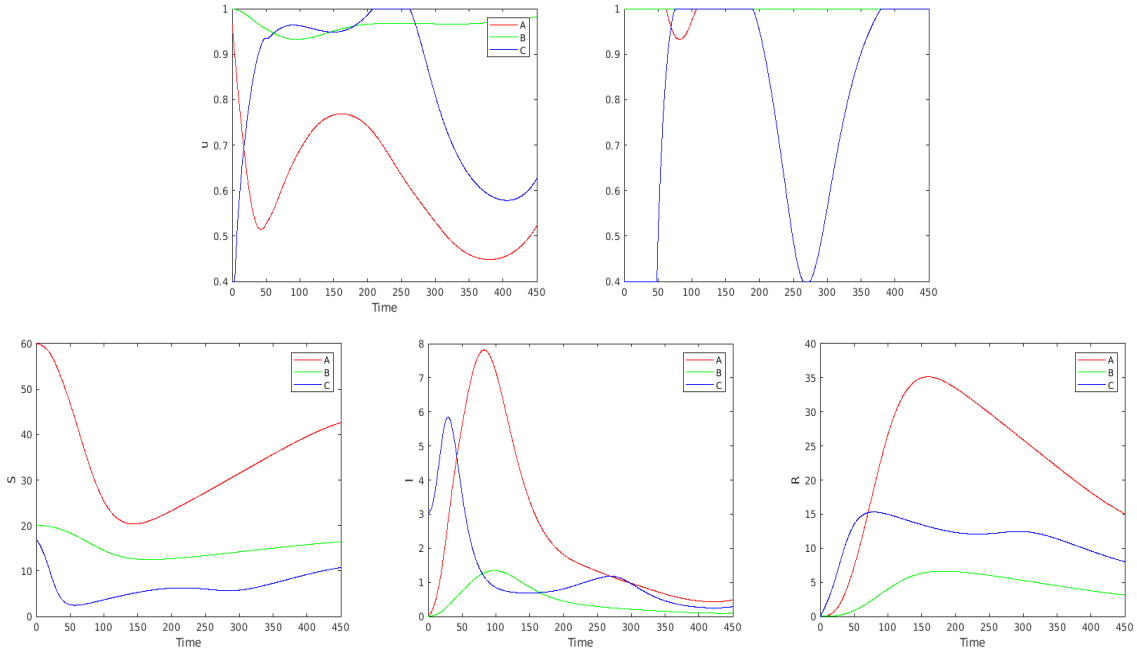


Figure 5.3: Optimization with respect to both $u$ and $v$ in the benchmark case. The fist two plots present the optimal controls $u$ and $v$, the second three plots give the corresponding $S$, $I$, and $R$.

**3.** The optimal control problem formulated in Section 4 is on a finite horizon. The question arises whether the optimal control substantially depends on the time horizon. This question is important for several reasons:

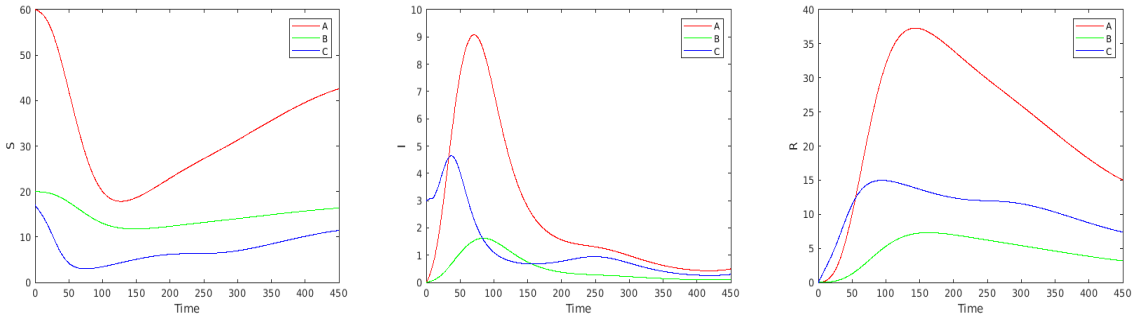


Figure 5.4: Optimization with respect to $u$ only (with $v = 1$) in the benchmark case. The plots present the trajectories of $S$, $I$, and $R$.

(i) It is natural to consider the optimization problem (2.5)–(2.7), (4.1) on the infinite horizon $[0, \infty)$, therefore the issue of convergence of the solution of the problem on $[0, T]$ when $T \to \infty$ is relevant (see the survey Aseev and Veliov [22] about this issue, in general).

(ii) In practice, any policy has to be revised in the course of application in order to catch up with new information. In particular, the improved medical understanding of the disease, changes in the death rates, new variants of the pathogens, etc. may emerge. Then the optimization problem has to be resolved (in an infinite or long horizon), and the optimal control has to be applied on a short horizon only, before the next update.

Figure 5.5 shows the optimal control $u$ for three time horizons. It is seen that the optimal controls are close to each other during the first about 50 days and are qualitatively similar in the first about 200 day. Thus updating the control every month (or less) is a reasonable choice in the framework of Model Predictive Control (MPC) based on new measurements. We mention that MPC (see e.g. Raković and Levine [23]) is the most widely applied method for real policy design in the context of epidemics, although its theoretical grounds seem not to be well adapted to this particular context in the existing literature on mathematical epidemiology.

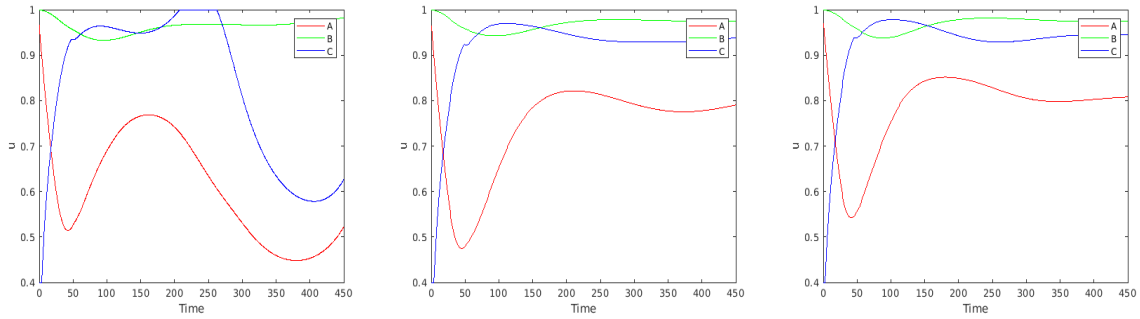


Figure 5.5: Optimal control $u$ for time horizon $T = 500$, 1000, 2000.

**4.** Comparative analysis: dependence on the activity rate of infected individuals $\alpha$, and on the contact rates $c$. First, we compare the optimal solutions for various values of the parameter $\alpha$. We remind that $\alpha$ can be decreased by increasing the testing effort. Only the size of the infected population is plotted in the first line of Figure 5.6, which shows that, as expected, the number of infected is increasing as $\alpha$ increases, the total number of deaths (second line, right) is increasing

correspondingly. The dependence of the total control "energy" $\mathcal{E}(x,\alpha) := \int_0^T (1-u(t,x))^2\,\mathrm{d}t$ (representing the social disutility), however, is more interesting. In the right plot on the second line of Figure 5.6 it is seen that the functions $\mathcal{E}(x_1,\cdot)$ and $\mathcal{E}(x_2,\cdot)$ (corresponding to locations $A$ and $B$) increase when $\alpha$ increases from 0.2 to the threshold $\alpha \approx 0.37$, after that they decrease. This fact can be explained by the effect of herd immunity. The higher the value of $\alpha$ above the threshold, the more people obtain immunity from infection and the effect of contact restriction becomes relatively smaller. The reduction of the control "energy" after the threshold, however, leads to a steep increase of the deaths.

Similar results are obtained when the multiplier $\hat{c}$ of the contact rates is varied, see Figure 5.7. For values of $\hat{c}$ above the threshold level $\hat{c} \approx 0.4$, the higher are the contact rates the less is the total of the applied control "energy", although the total number of deaths increases faster. This means that for populations with intensive contacts between people the optimal contact restrictions are low; the optimizing decision maker relies more on the herd immunity.

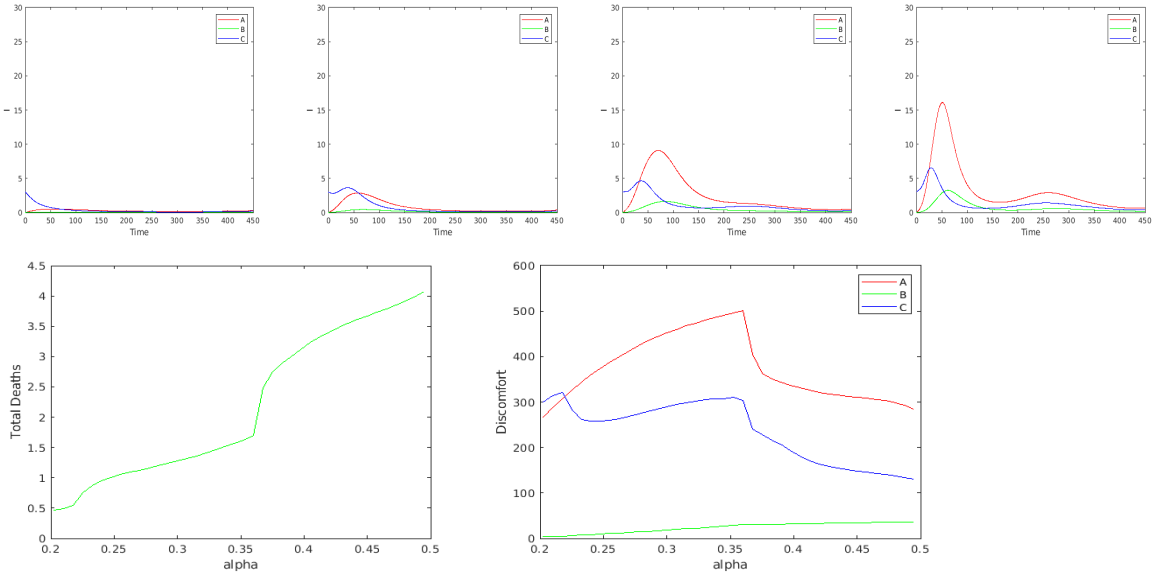


Figure 5.6: Infected population in the optimal solution for values of $\alpha = 0.2, 0.3, 0.4, 0.5$ (first line), total number of deaths (second line left), and total "control energy" $\mathcal{E}$ (second line right)—called "discomfort" on the plot—on $[0,T]$ as functions of $\alpha$.

**5.** Finally, we investigate the dependence of the optimal contact restrictions $u$ on the discount rate $r$. It is remarkable that the control effort considerably increases with the discount rate, see Figure 5.8. The explanation of this fact is not obvious, because one can expect the opposite: higher $r$ means higher discount of the deaths in the future, hence less control action is required. However, higher $r$ also means that the future control and economic costs are more discounted, thus of lower value. The results on Figure 5.8 show that the second effect dominates. Indeed, a discount factor $r = 0.00075$, for example, leads to approximately 56% decrease of value in 3 years, which is reasonable for the deaths, because one can expect a substantial progress of medication and medical service in three years, while the purely economic discount factor is normally much lower: about $0.03/365 = 0.00008$. In a model with a more realistic representation of the economic losses,

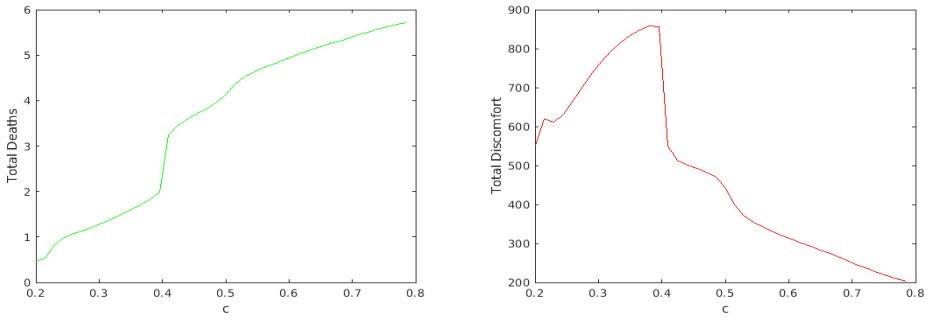


Figure 5.7: Total number of deaths (left plot) and total social disutility (right plot) in the optimal solution for multiplier $\hat{c} = 0.2,\ 0.4,\ 0.6,\ 0.8$ of the contact rates.

the humanitarian and the economic components in the objective functional have to be differently discounted.

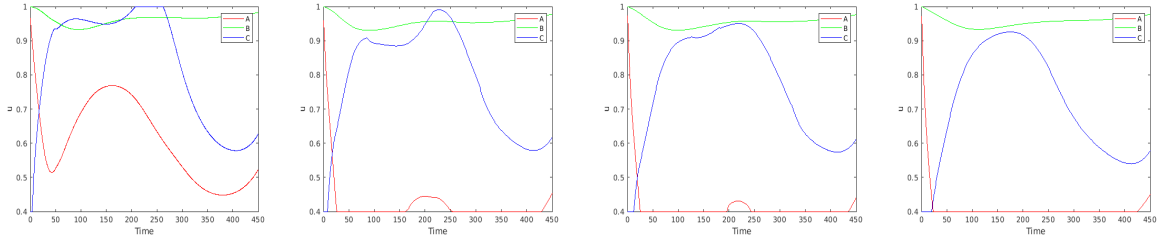


Figure 5.8: Optimal controls $u(\cdot, x)$ for values of discount $r = 0,\ 0.00075,\ 0.0015,\ 0.0030$.

# 6 Discussion

We develop a spatiotemporal epidemiological model and focus on the investigation of human contact and mobility restrictions. The novel element of our work is the control theoretical approach to optimization of the policies. As a preliminary step we obtain conditions for stability of the disease free equilibria, and an explicit formula for the basic reproduction number.

The contact and mobility restrictions, the latter in form of partial lock-down, are considered as control variables representing the policies. The optimal control problem aims at minimization of an intertemporal combination of three components: the total number of deaths (or hospitalizations) due to the epidemic, the socio-economic cost of the policy measures, and the economic losses due to the epidemic and the partial lock-downs.

The particular scenarios studied in the paper involve three locations (e.g. cities) and the contact and mobility restrictions within and between them. We investigate the effects of the restrictions also in association with other measures such as the intensity of testing whether individuals are positive to the infection status.

Numerical results show various effects concerning the optimal policies and the evolution of the epidemic. It is shown that in case of a disease with relatively long incubation period in part of which infected individuals are infectious, testing (leading to smaller labour participation of infected individuals (LPI)) is crucial, especially in suppressing the firs wave of the epidemic.

There is a threshold of the LPI value below of which higher LPI leads to more restrictions at the optimum, and above which higher LPI leads to less restrictions accompanied, however, with a steep increase of deaths. The heard immunity is more efficient than restrictions in the latter case. Similar threshold effect is observed for the dependence of the optimal contact restriction policy on the natural contact rates of the population. The numerical results also indicate that the optimal policy restricted to a relatively short initial interval does not substantially depend on the time horizon in which the optimization problem is solved. This allows for application of the model predictive control method for policy update based on current measurements. Interesting properties of the timing and intensity of the contact restrictions in different locations are obtained, depending on the flows of people between the locations.

Overall, the paper provides useful insights into optimal control of outbreaks. Besides other spatial intervention scenarios, several extensions of the approach are possible: more detailed epidemiological models including additional compartments such as exposed, asymptomatic infected, isolated, etc. Moreover, existing models involving vaccination, waning immunity, etc., can be embedded into spatial framework similarly as in the present paper. More interesting from mathematical point of view is an extension with a distributed (not necessarily discrete) space. This leads to models in which the population compartments are represented by measures instead of finite-dimensional points. Optimal control problems in spaces of measures are currently under intensive investigation.

An extension would be the analysis of epidemic models to be accompanied by optimal control approaches in other societal areas. In particular at the socio-economic level, this is important since the implications of emerging health threats such as pandemics are not only in terms of public health but also critically affects other areas of society, the disruption of which may in turn have again consequences on public health.

## Data availability statement

All data supporting the findings of this study are available within the paper.

## Disclosure statement

The authors declare there are no competing interests.

## References


[1] Hethcote HW. Modeling heterogeneous mixing in infectious disease dynamics. In Models for Infectious Human Diseases, V. Isham and G. F . H. Medley, eds., Cambridge University Press, Cambridge, UK, 1996; p. 215-238

[2] Brauer F, Castillo-Chavez C, Feng Z. Mathematical models in epidemiology. 2019, Vol. 32, Springer, Berlin

[3] Castillo-Chavez C, Bichara D, Morin BR. Perspectives on the role of mobility, behavior, and time scales in the spread of diseases. Proc Natl Acad Sci. 2016; 113(51):14582–14588

[4] David JF, Iyaniwura SA, Ward MJ, Fred B. A novel approach to modelling the spatial spread of airborne diseases: an epidemic model with indirect transmission. Math Biosci Eng. 2020; 17(4):3294–3328

[5] David JF, Iyaniwura SA. Effect of human mobility on the spatial spread of airborne diseases: An epidemic model with indirect transmission. Bull Math Biol 2022; 84:63

[6] Zhang F, Jin Z. Effect of travel restrictions, contact tracing and vaccination on control of emerging infectious diseases: transmission of COVID-19 as a case study. Math Biosci Eng. 2022; 19(3):3177-3201

[7] Bertaglia G, Boscheri W, Dimarco G, Pareschi L. Spatial spread of COVID-19 outbreak in Italy using multiscale kinetic transport equations with uncertainty. Math Biosci Eng. 2021; 18(5):7028-7059

[8] Chen D, Xue Y, Xiao Y. Determining travel fluxes in epidemic areas PLoS Comput Biol 2021; 17(10):e1009473

[9] Geng X, Katul GG, Gerges F, Bou-Zeid E, Nassif H, Boufadel MC. A kernel-modulated SIR model for COVID-19 contagious spread from country to continent. PNAS 2020; 118(21):e2023321118

[10] Grimee M, Bekker-Nielsen Dunbar M, Hofmann F, Held L. Modelling the effect of a border closure between Switzerland and Italy on t e spatiotemporal spread of COVID-19 in Switzerland. Spatial Statistics 2021; 49:100552

[11] Aguilar J, Bassolas A, Ghoshal G, Hazarie S, Kirckley A, Mazzoli M, MeloniS, Mimar S, Nicosia V, Impact of urban structure on infectious disease spreading. Sci Rep. 2022; 12:3816

[12] Jia Q, Li J, Lin H, Tian F, Zhu G. The spatiotemporal transmission dynamics of COVID-19 among multiple regions: A modeling study in Chinese provinces. Nonlinear Dyn. 2022;107:1313-1327

[13] Rapti Z, Cuevas-Maraver J, Kontou E, Liu, Drossinos Y, Kevrekidis PG, Barmann M, Chen QY, Kevrekidis, GA. The role of mobility in dynamics of the COVID-19 epidemic in Andalusia. Bull Math Biol. 2023;85:54

[14] Mazzoli M, Pepe E, Mateo D, Cattulo C, Gauvin L, Bajardi P, Tizzoni M, Hernando A, MEloni S, Ramasco JJ. Interplay between mobility, multi-seeding and lockdowns shapes COVID-19 local impact. PLoS Comput Biol. 2021; 17(10) e1009326

[15] Parino F, Zino L, Porfini M, Rizzo A. Modelling and predicting the effect of social distancing and travel restrictions on COIVD-19 spreading. J Royal Soc Interface 2021; 18:20200875.

[16] Topirceanou A, Precup R-E. A novel geo-hierarchical population mobility model for spatial spreading of resurgent epidemics. Sci Rep. 2021; 11:14341.

[17] Schoot Uiterkamp MHH, Goesgens M, Heesterbeck H, van der Hofstad R, Litvak N. The role of inter-regional mobility in forecasting SARS-CoV-2 transmission. J R Soc Interface 2022; 19:20220486.

[18] Nakata Y, Roest G. Global analysis for spread of infectious diseases via transportation networks. J Math Biol. 2015; 70:1411-1456

[19] Bloom DE, Kuhn M, Prettner K. Modern infectious diseases: macroeconomic impacts and policy responses. PGDA Working Paper No. 27757, 2020.

[20] Caulkins JPP, Grass D, Feichtinger G, Hartl RF, Kort PM, Prskawetz A, Seidl A, Wrzaczek S. The optimal lockdown intensity for COVID-19. J Math Econ. 2021; 93:102489

[21] Dontchev AL, Hager WW, Veliov VM. Second-order Runge-Kutta approximations in control constrained optimal control. SIAM J Num Anal 2000; 38(1):202–226

[22] Aseev SM, Veliov VM. Another view of the maximum principle for infinite-horizon optimal control problems in economics. Russ Math Surv. 2019; 74(6):963–1011

[23] Raković S.V., Levine W.S., Eds. Handbook of Model Predictive Control. 2018. Birkhäuser.